An Investigation of the Mechanical Filtering Effect of Tactile CMM in the Measurement of Additively Manufactured Parts

S. Lou[1], S. B. Brown[2], W. Sun[2], W. Zeng[1], X. Jiang[1*], P. J. Scott[1]

[1] EPSRC Future Metrology Hub, University of Huddersfield, Queensgate, Huddersfield, HD1 3DH, UK

[2] National Physical Laboratory, Engineering, Materials and Electrical Science, Hampton Road, Teddington, Middlesex, TW11 0LW, UK

*Corresponding author: x.jiang@hud.ac.uk

Abstract

The high level of surface roughness of additively manufactured parts post challenges to the applicability of different dimensional measurement techniques, including tactile, optical and X-ray computed tomography. Tactile measurement is traditionally considered to have the best accuracy and traceability; however, its measurement can be significantly influenced by the mechanical filtering effect. This work investigates the influence of the mechanical filtering effect on tactile measurements of additively manufactured parts. Both experimental and simulation work are utilised to reveal this effect. Particularly the numerical simulation based on the morphological method allows a single influence factor e.g. the stylus diameter to be investigated. The maximum measurement errors caused by the stylus mechanical filtering effect are determined by the convex hull points of the measurement profile, which is equivalent to using an infinitely large stylus. Coordinate measuring machine and X-ray computed tomography measurement results of an additively manufactured test part's cylinder diameters are compared, along with the application of morphological method to "compensate" the coordinate measuring machine's mechanical filtering effect.

1. Introduction

Building up a component layer by layer, via additive manufacturing (AM), allows the construction of complex geometries not possible with conventional manufacturing processes. However, an insufficiency of AM is its poor surface finish with roughness ranging from a few micrometres to several hundreds of micrometres. This high surface roughness of AM parts post challenges to the applicability of different dimensional measurement techniques, including tactile, optical and X-ray computed tomography (XCT).

Tactile measurement techniques, e.g. coordinate measurement machines (CMMs) coupled with tactile probes, are traditionally considered to have a good level of accuracy and traceability. However, a tactile measurement can be significantly affected by the interaction of the stylus tip and the surface texture, this is known as the mechanical filtering effect (Whitehouse 2002; Thomas 1999). Optical sensors were also found to be significantly affected by the level of surface roughness, making accurate determination of the position of the surface hard to achieve. Moreover, tactile and optical techniques are not able to measure some of the complex AM geometries, whose intricate forms do not permit line-of-sight. In contrast, XCT can measure both internal and external surfaces of such objects (Carmignato et al. 2018); however, the systematic errors, when employing XCT as a dimensional measurement technique, are not fully understood. Although an international interlaboratory comparison of XCT systems shows that most of XCT dimension

measurement achieved sub-voxel accuracy, traceability of XCT dimensional measurement is still a major challenge (Carmignato 2012).

Both tactile and XCT measurement feature surface filtering effects, although different characteristics. The effects of the mechanical filtering of tactile stylus are well-known (Lonardo et al. 2002). Tactile measurement is via the physical contact of the tactile stylus and the surface under measurement. Due to the finite size of stylus, it is unable to access some deep valleys, and thus the measured surface is not the true surface but an approximate one, i.e. the mechanical surface (Weckenmann et al. 2004; Leach & Haitjema 2010; ISO 3274 1996). XCT does not have the limitation of mechanical filtering effect. If sufficiently small voxel size compared to measured surface texture and sufficiently small focus spot size are available for XCT measurement, e.g. nano XCT systems, XCT can theoretically measure short wavelength components of surface texture, allowing the virtual probing of sharp valleys on surfaces (Aloiso & Carmignato 2016). However, in reality the XCT system, due to its measurement principles and hardware, also generates a low-pass filtering effect, where both surface peaks and valleys are smoothed (Kruth et al. 2011; Carmignato et al. 2017). The averaging effect is caused by the partial volume effect (PVE) of the XCT system, which refers to the 3D image blurring/fuzziness introduced by the finite spatial resolution of the XCT imaging system and image sampling (Soret et al. 2006, VGStudio Manual).

There is a current lack of international standards covering the dimensional verification and traceability of XCT. XCT measurements often refer back to tactile probing as the reference data, e.g., CMMs with tactile stylus, due to the fact that tactile CMMs can provide traceable measurements and well-established ISO standards are available for its performance verification (ISO 10360-2 2009). However, when using the tactile reference for XCT, it should be noted that tactile probing does not measure real surface, especially in the case of rough surface texture, e.g. AM surfaces. Normally the rougher the surface is, the more obvious the mechanical filtering effect will be. The confidence associated with the individual measuring techniques when measuring traditionally machined parts bearing smooth surfaces cannot be directly translated across to AM parts, where the surface roughness (as well as other factors) appear to influence the result (Brown et al. 2016).

Comparisons of tactile and XCT dimensional measurements on rough surfaces are available from recently published works. Schmitt and Niggemann (2010) estimated that the influence of surface texture on the XCT measurement is approximately *Rz*/2. Similarly, Bartsher et al. (2010) stated that the surface roughness contributes to uncertainty of measurements in the order of *Rz*/2 as an upper limit. For their experimental case, the effect was estimated to be less than *Rz*/4. From the experiments of Boeckmans et al (2015), the offsets between XCT and tactile measurement were in 1:1 ratio of the *Rp* value. Brown et al. (2016) conducted an experimental comparison using various dimensional measurement systems to measure AM metallic parts, these comparisons inferred there were systematic measurement differences between the different measuring systems. Salzinger et al. (2016) fabricated an aluminium hollow shaft with rough surfaces; measurement results showed that as the diameter of CMM probing tip increases, the measured diameters of the outer hollow cylinder increase. In comparison, the measured diameters of the inner cylinder decrease with increasing tip diameter. It was also found that both the outer and inner diameters measured by XCT decrease as the voxel size increases. A similar experimental work can refer to Novak and Runje (2017). Aloisi and Carmignato (2016) provided an experimental investigation on the influence of surface roughness on XCT dimensional measurements of AM parts. They found that the deviations between CMM and XCT in measuring AM cylinder diameters are approximately *Rz*/2. In particular, external diameters obtained by XCT measurement are

smaller than the corresponding CMM reference values of approximately *Rz*/2, while for internal diameters the results are the reverse. Carmignato et al. (2017) further conducted a simulation study to investigate the XCT's filtering effect on dimensional measurements of components with rough surfaces, which shows that the mean deviations (between least-squares diameters and reference diameters of simulated cylinders) of 2*Rp* take place independently from surface roughness; the authors also investigated the influences of voxel sizes, XCT surface determination algorithms, focus spot and fitting operations on dimensional measurements. It is noted that the *R* parameters used in the aforementioned literature should refer to the *P* parameters according to ISO 4287 since the filtration techniques are not applied and the whole surface texture has impact on tactile measurement.

Although the mechanical filtering of tactile probing is well known, the evaluation of its influence on dimensional measurement is mainly based on hardware experiments, for instance, geometrical dimensions are measured by CMM using various sizes of tactile probe styluses. This paper systematically evaluates the influence of the mechanical filtering effect on dimensional measurement of AM processed components, while the exploration of XCT filtering effect is scheduled for a separate publication. Experiments are designed to verify the mechanical filtering effect. An AM test object will be measured by a CMM with various stylus tip diameters. Numerical simulation will be utilised to mathematically simulate the tactile scanning process. The simulation is used because a number of parameters can influence the metrological performance of the tactile measuring system, e.g., length of stylus, probing force, weight of stylus, scanning speed, probing direction (Christoph and Neumann 2012). Numerical simulation allows the isolation of a single influence factor, e.g. the stylus diameter in this work. To distinguish the physical probe used in the experiments and the simulated probe used in the numerical simulation, the former is called the "stylus probe" and the latter is called the "disk probe".

The paper is laid out in the following format: Section 2 looks into the details of the mechanical filtering effect. Section 3 describes the experimental work of measuring the designed AM test object. Section 4 provides the numerical simulation of tactile scanning process using the morphological method. Section 5 presents the comparison of the measurement result of CMM and XCT, including the application of the morphological method to XCT measured profile. Section 6 reaches the conclusion.

2. Mechanical filtering effect

The scanning of the workpiece surface using a tactile probe, e.g. the analogue probe or the touch trigger probe, is a common practice in geometrical measurement and a hardware implementation of the morphological dilation operation (Krystek 2004; Lou et al. 2014a). The workpiece surface as the input set is dilated by the structuring element (the stylus tip) to generate the morphological output (the measured surface), which is also called the traced surface. The scanning measurement is conducted by traversing the tip over the surface. The tip centre coordinates are recorded at each sampling position; these coordinates are then used to give a discrete representation of the measured surface. In ISO 3274 (1996), the traced surface profile is defined as "*locus of the centre of a stylus tip which features an ideal geometrical form (conical with spherical tip) and nominal dimensions with nominal tracing force, as it traverses the surface within the intersection plane*".

In common practice, the stylus employed for scanning are small in size. However, the finite size of stylus still influences the precision measurement of workpiece surfaces. Figure 1 demonstrates the effect of traversing the stylus over the workpiece surface. By comparing the traced profile with the real workpiece profile, it is evident that the stylus tip tends to round

off peaks on the profile making it broader, nevertheless the peak height remains constant. The valleys on the profile are smoothed by the tip becoming narrow, meanwhile the valley height is reduced (Dagnall 1998). This effect introduces distortion into measurement of workpiece surfaces and is called the mechanical filtration effect of tips. For the measurement of workpiece surfaces, especially for freeform shaped workpieces, the distortions caused by the tip mechanical filtration effect appreciably influences measurement accuracy. Correction to the traced surface is desired in order to restore to the real workpiece surface. However, the traced surface is unable to be perfectly reconstructed to the real surface, but only to an approximation of the real mechanical surface. This is due to the nonlinearity of morphological operations.

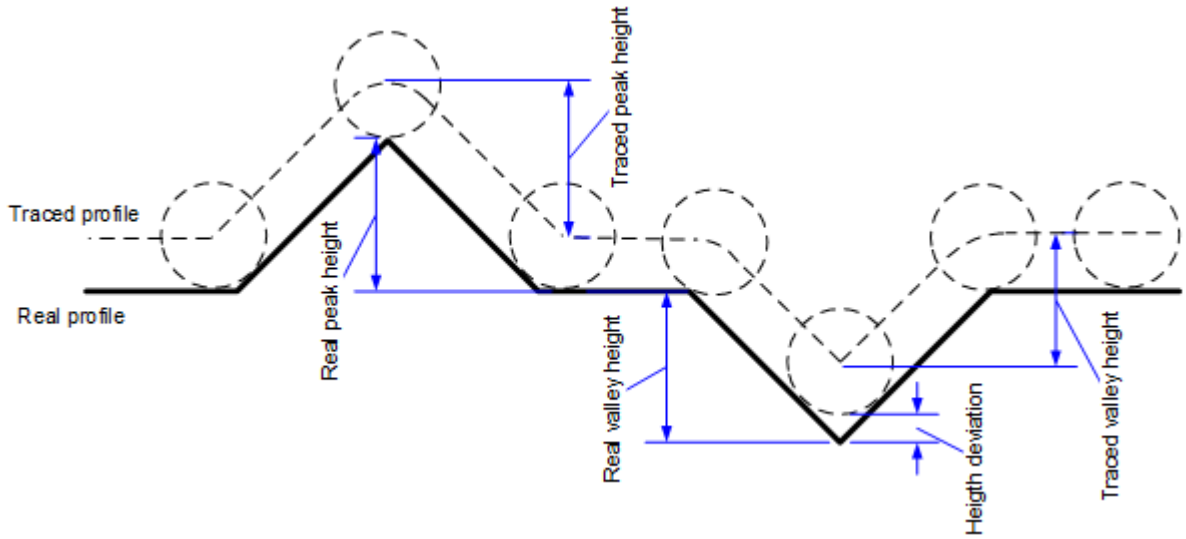

Figure 1. Tip mechanical filtering effects.

ISO 14406 (2003) presents the definition of mechanical surface: "*boundary of the erosion, by a sphere of radius r, of the locus of the centre of an ideal tactile sphere, also with radius r, rolled over the real surface of a workpiece*." Figure 2(a) presents the traced profile, while Figure 2(b) illustrates the reconstruction process. An ideal sphere with the same size to the stylus tip is rolled over the traced profile from below. The locus of the centre of this ideal sphere is regarded as the mechanical surface. Rolling the sphere below the traced surface, is mathematically equivalent to applying an erosion operation on the traced surface using a spherical structuring element.

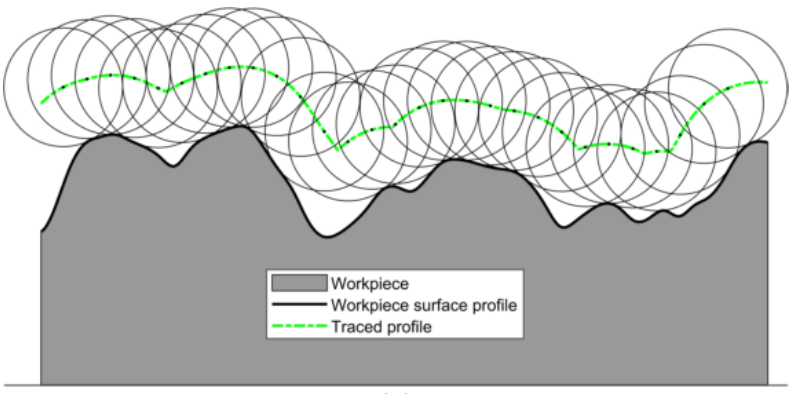

(a)

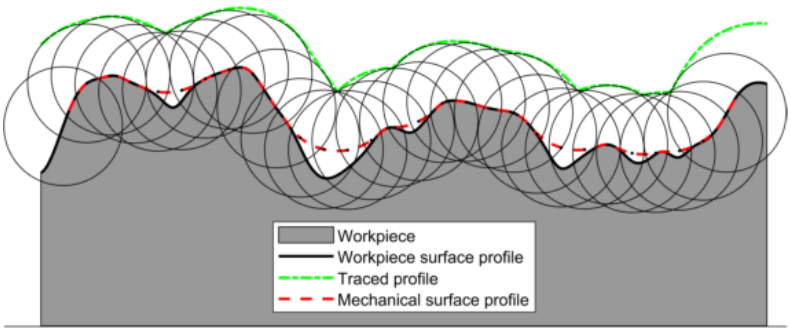

(b)

Figure 2. Reconstruction of mechanical surface: (a) traced profile; (b) reconstructed mechanical surface.

The morphological erosion operation cannot recover the original real surface perfectly due to the nonlinearity of morphological operations. Morphological operations can only reconstruct those surface portions where the local surface curvatures are larger than that of the stylus tip (Krystek 2004; Roger et al. 2005). This implies that the real mechanical surface differs from the real surface at the locations where the local surface curvature is smaller than the tip. Thus, the reconstructed real mechanical surface varies with the stylus tip size, Figure 3 presents such an example. Large stylus tips tend to reduce and smooth the surface irregularities, while small tips enable the reconstructed surface to better approximate the real surface.

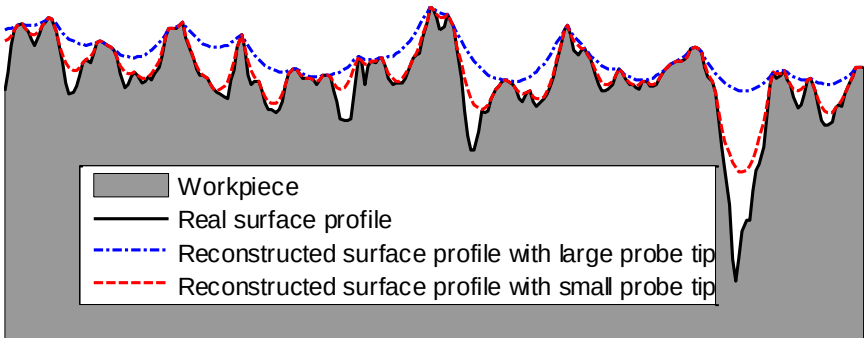

Figure 3. Reconstructed real mechanical surfaces vary with the tip size.

3. Experimental analysis

3.1 AM test object

An AM test object was designed at the National Physical Laboratory (NPL) and built at University of Birmingham by Selective Laser Melting (SLM) using AlSi10Mg powder. The test object is aimed to assist in the investigation of the performance of different dimensional measurement tools on measuring AM components. It incorporates both external and internal features that are accessible by traditional measuring systems, such as CMMs. The designed geometrical features have simple forms (e.g. cylinders, flats and cubes) that can be easily characterised. See Figure 4.

The AM test object is attached to a removable aluminium base plate. To ensure a repeatable and positive fit to the base plate, the base of the AM test object has been ground flat and orthogonal to the intersection of two adjacent sides of the AM test object. The base plate includes three ceramic tooling spheres. The positions of these spheres allow a unique coordinate system to be generated and the distance between the spheres allows a verification of scale. Being precision spheres, the measurement of the surface and the

determination of its centre, using the applied least-square (LS) best fit routines, should result in low standard deviation. The same three spheres were used to provide a scale reference for the comparison of tactile and XCT measurements.

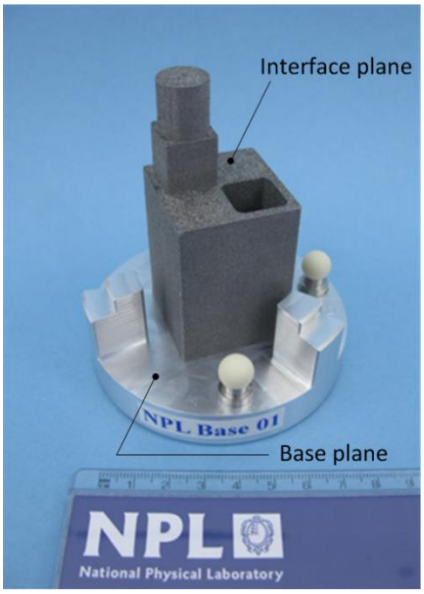

Figure 4. NPL AM test object fitted into a base plate with three ceramic tooling balls.

3.2 Tactile measurement of NPL AM test object

Measurements of the AM test object and base plate were made on a Mitutoyo Crysta Apex – C 7106 CMM, with a maximum permissible error (MPE) = (1.7+3L/1000) µm, where L is measured in mm. A set of measurements were repeated using tooling spheres of: 3 mm, 4 mm and 5 mm in diameter, using a Renishaw PH10MQ motorised indexing head, fitted with the SP25-M touch-trigger scanning probe system and the three different diameter attachments.

Each set initially measured the three tooling spheres to generate a coordinate system and the top of the base plate. Measuring the top of the base plate allows a base plane to be defined. This base plane, defined as the ‘Base plane’ in Figure 4, in theory is the same plane that the base of the AM test object possesses. This universal plane allows height measurements made to the AM test object on and off the base plate to be compared.

A plane, named the ‘Interface plane’, was defined at the interface of the internal and external features, see Figure 4. This interface plane was measured using approximately 300 points, and defined using a least-squares (LS) algorithm. The distance between this plane and the base plane of the AM test object was calculated, allowing an examination of plane offsets caused by the effect of surface roughness.

The cylinder’s circumferences were measured at different heights: 23.5 mm, 26 mm, 28.5 mm, 31 mm for the internal cylinder, and for the external cylinder at: 68 mm, 70.5 mm, 73 mm and 75.5 mm, all from the base plane datum. Measuring the circle positions from the base plate plane minimizes any offset, due to surface roughness, that may be caused if the interface plane of the AM test object had been used as the datum plane.

Each of the circles measured using the three different diameter stylus probes, was generated using a minimum of two thousand points. The points were measured while scanning the surface, the speed of the scan was kept constant at 3.0 mm/s, and a probing

force calculated from the manufacturer's information. A LS best fit algorithm was used to define the circle diameter and associated standard deviation at 1 sigma.

3.3 Measurement results

The height of the interface plane is defined as the distance between two points; the point defined as the intersection of the internal cylinder's axis with the interface plane and the point defined by the intersection of the axis of the same cylinder and the base plane. It is assumed that the cylinder axis will not change by any significant amount. This is due to the fact that although the cylinder diameter may change, the centre will not, as the topography of the surface is assumed to be random and thus dilation/erosion is from a central point.

The interface plane heights are listed in Table 1 and plotted in Figure 5. It can be seen that the distances increase with increasing stylus diameters. This conforms to the theoretical analysis that the larger the tip diameter, the closer the measured profile approaches to the profile peaks. The distance offsets between the 3 mm stylus and the 4 mm stylus, the 4 mm stylus and the 5 mm stylus are 14 μm and 11 μm respectively.

Table 1. Interface plane heights in response to three tip diameters of the stylus probe (Unit: mm).

Tip diameter	Interface plane height	Base plane height	Distance
3	38.800	-9.992	48.792
4	38.799	-10.007	48.806
5	38.826	-9.991	48.817

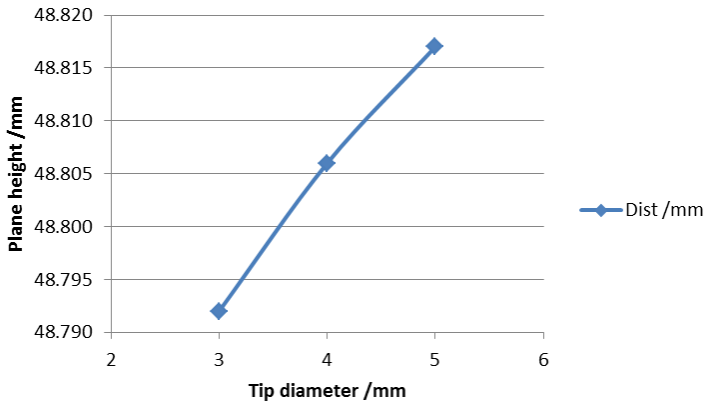

Figure 5. Variation of top plane heights in response to the stylus tip diameters.

The measurement results of the external and internal cylinder diameters are listed in Table 2 and Table 3 and plotted in Figure 6 and Figure 7 respectively. It is observed that all four external cylinder diameters increase with increasing tip diameter, while all four internal diameters decrease with the increase of tip diameter.

Table 2. External cylinder diameters in response to varying tip diameters of the stylus probe (Unit: mm).

surface height / Tip diameter	68.0	70.5	73.0	75.5
3	14.052	14.040	14.060	14.056
4	14.073	14.058	14.078	14.075
5	14.082	14.066	14.088	14.085

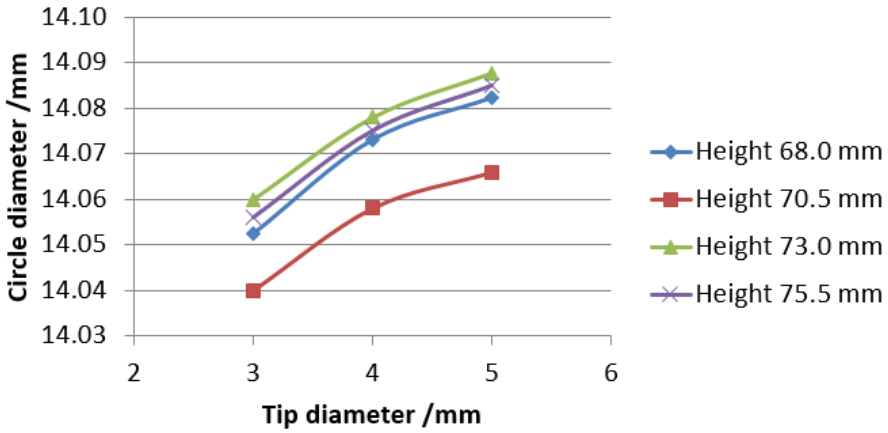

Figure 6. Variation of external cylinder diameters in response to stylus tip diameters.

Table 3. Internal cylinder diameters in response to varying tip diameters of the stylus probe (Unit: mm).

surface height / Tip diameter	23.5	26.0	28.5	31.0
3	13.721	13.716	13.727	13.755
4	13.688	13.687	13.701	13.725
5	13.676	13.672	13.682	13.716

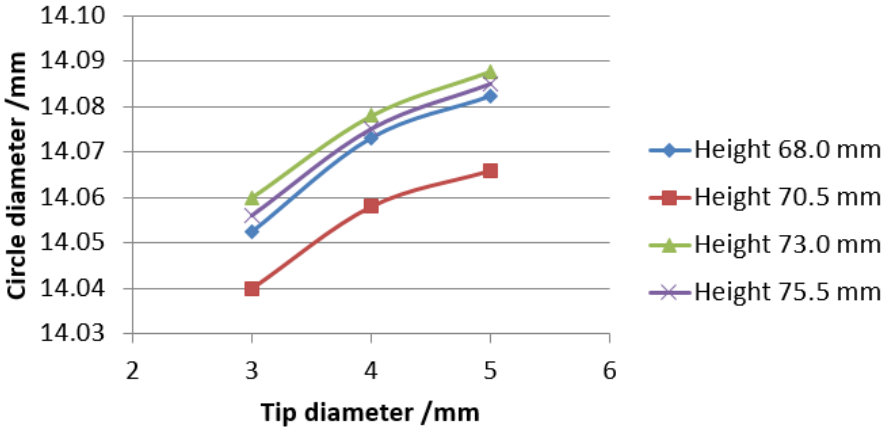

Figure 7. Variation of internal cylinder diameters in response to stylus tip diameters.

4. Numerical simulation by morphological method

4.1 Morphological method based on the Alpha shape theory

Mathematical morphology is a mathematical subject that examines the geometrical structure of an image by matching it with small patterns at various locations in the image. By varying the size and the shape of the matching patterns, called the structuring elements, one can extract useful information about the shape of the different parts of the image and their interrelation (Heijmans 1995). Four basic morphological operations, namely dilation, erosion, opening and closing, form the foundation of mathematical morphology.

Morphology operations enable the numerical simulation of the mechanical filtering effect of of tactile CMM. The use of morphological method to reconstruct the mechanical surface has been adopted in high precision nanometre scale surface measurements, e.g. Atomic Force Microscopy (Villarrubia 1997; Qian & Villarrubia 2007). The adopted algorithms in this work were based on morphological image processing techniques where the measured surface height map is treated as a grey-scale image; however, where the surface is curved, these approaches are no longer valid. Recent computational methods based on the Alpha shape theory have removed this limitation (Lou et al. 2013b; Lou et al. 2014).

The developed Alpha shape method was constructed based on the relationship that the Alpha hull is equivalent to morphological closing and opening envelopes with circular structuring element (Worring and Smelders 1994). This theoretical link enables the computation of closing and opening operations on arbitrary shapes of surfaces without the limitation of the image processing based methods. The Alpha shape method is based on the Delaunay triangulation from which the boundary facets of the alpha shape are extracted. See Figure 8 for an example of computing the closing envelope of a cylinder circumference profile, where the inner and outer facets of the Alpha shape are separated according to their normal vectors. In the example, the normals of outer facets point to outside of the roundness profile and these facets are to be used to determine the closing envelope which is equal to the associated Alpha hulls.

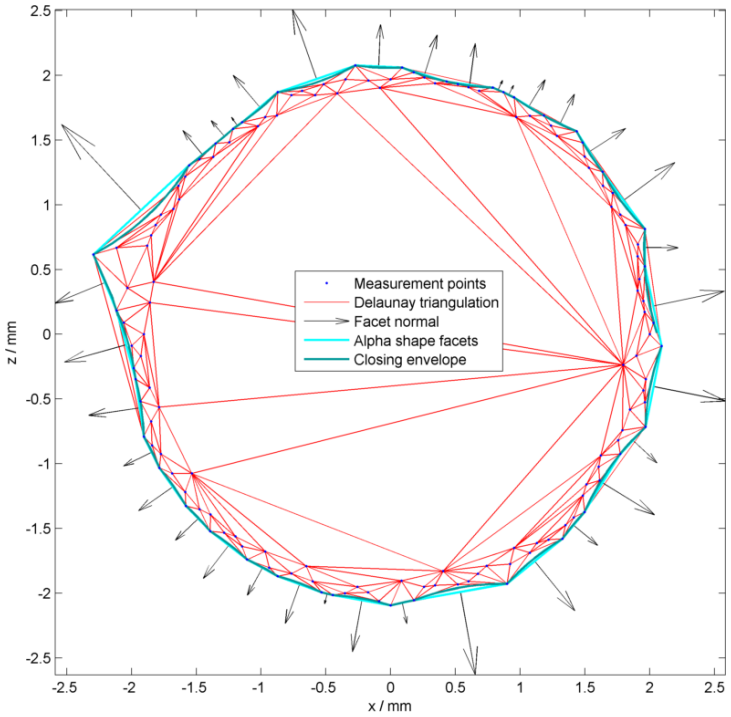

Figure 8. The morphological filtering on the cylinder circumference profile based on Alpha shape algorithm.

4.2 Simulation: varying disk probe diameters

Using the Alpha shape method, a numerical simulation is designed to investigate the mechanical filtering effect of tactile CMM. The designed simulation comprises two cases, i.e. scanning a measured AM planar profile and a wrapped AM round profile using different disk probe diameters. The former case is used to examine the distance offset while the latter is used for the investigation of dimension offset.

In the first case, the profile was measured from the interface plane of the NPL test object using Taylor Hobson profilometer with the stylus tip radius 2 µm. The resultant relevant surface texture profile parameters are *Pa* 38.4 µm, *Pq* 51.8 µm, *Pp* 211.9 µm and *Pz* 339.8 µm. The profile is levelled but not filtered since the whole surface texture has impact on tactile probing. The disk probe diameters range from 0.3 mm to 12 mm. Figure 9 presents three closing envelopes of 3 mm, 4 mm and 5 mm disk probe diameters respectively and the corresponding Gaussian least-square planes of these disk probe diameters. It can be seen, from Figure 9, the larger the disk probe diameter, the more the envelope approaches the profile peak portions and, thus, the greater the offset in height. The lines representing the *Pp* and *Pz*/2 height plane are also marked in Figure 9 to indicate the limits of height offset. For planar surfaces, the extreme case, where the disk probe is infinitely large, will produce the largest offset, *Pp*. Nonetheless, the height offset produced by the 3 mm, 4 mm and 5 mm disk probes are within this limit and much smaller than *Pp*; being around 6% of *Pp*. The *Pz*/2 plane is 42 µm below the *Pp* plane, which indicates that the largest valley is smaller than the largest peak in amplitude. If these two are with the same amplitude, then the *Pp* and *Pz*/2 plane would overlap.

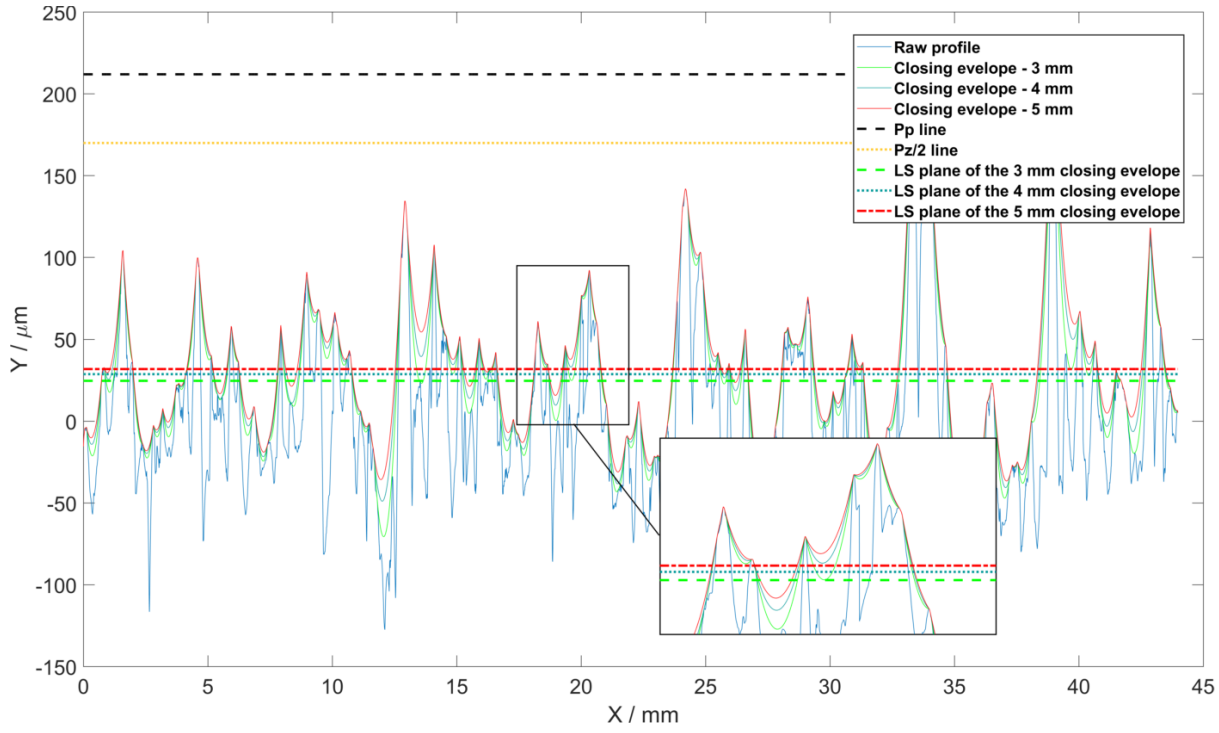

Figure 9. Closing envelopes of different disk radii (3 mm, 4 mm and 5 mm) and various limiting planes.

In the second case, the previous AM profile was wrapped around a circle of diameter 14 mm. Figure 10 shows the closing envelope of a 5 mm disk, which is used to present the numerical simulation of scanning the circumference of an external cylinder (diameter: 14 mm). Please note that the round profile diameter is suppressed by 13 mm to enable a better visualisation of surface texture. The LS diameter, from the closing envelope, is slightly larger than that of the original stylus measured profile, indicating the offset effect of the disk probe diameter to dimension measurement. In the extreme case of using an infinitely large disk probe diameter, the probe tip will only contact a limited number of points on the profile. Theoretically these contact points are the vertices of the convex hull of the round profile. The green circle in Figure 10 marked the LS circle produced by the convex hull points. The diameter of this green circle, rather than the diameters of the *Pp* and *Pz*/2 circles, is the limit that a probe diameter can produce, and should be smaller than the *Pp* circle.

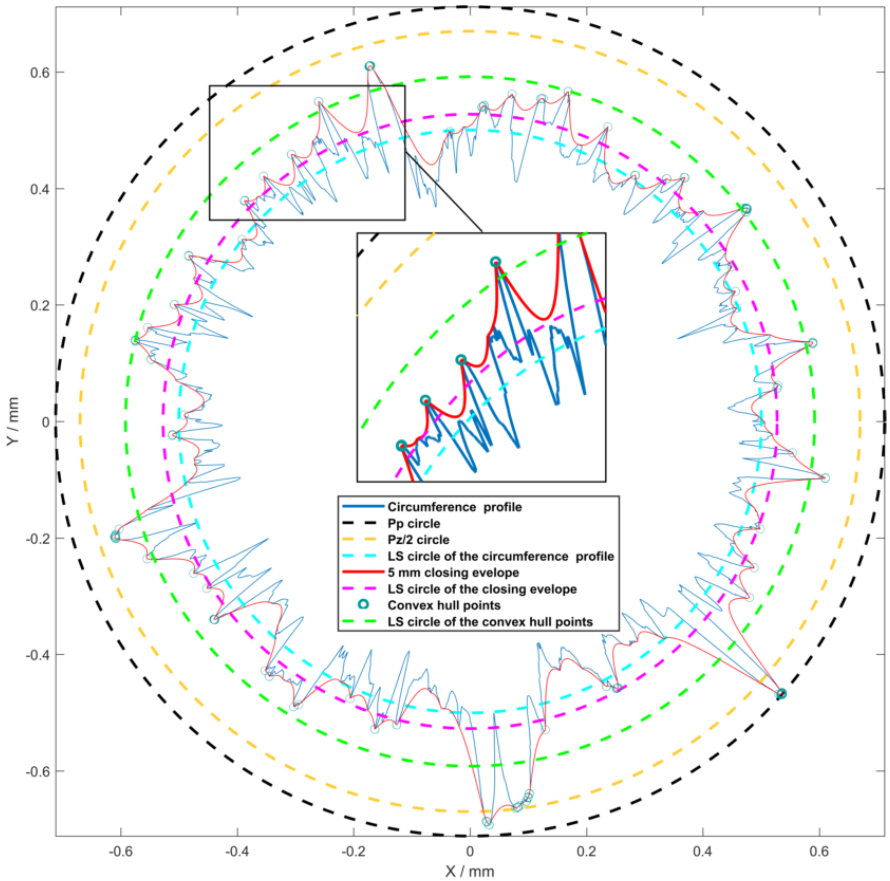

Figure 10. Closing envelope of the 5 mm disk and various limiting circles.

The full results of applying the whole set of disk probe diameters are listed in Table 4 and plotted in Figure 11. The external cylinder diameters are obtained by rolling the disk from the outside of the circumference profile. Similarly, the internal cylinder diameters are obtained by rolling the disk from the inside of the same profile. It can be seen that larger probe diameters produce a greater offset from the true surface profile in both plane heights and cylinder diameters. This offset due to probe diameter, results in the diameter of the external cylinder

increasing with an increase of probe diameter and the diameter of the internal cylinder decreasing with an increase in probe diameter. The offset diameter will gradually approach the limit, namely the one determined by the convex hull points.

Table 4. Plane height offset and external/internal cylinder diameters resulted from a set of disk probe diameters.

Disk probe diameter /mm	Plane height offset /µm	External cylinder diameter /mm	Internal cylinder diameter /mm
0.3	3.1	14.001	14.000
0.5	5.5	14.001	14.000
0.7	7.9	14.002	13.999
1	11.7	14.003	13.998
1.5	16.1	14.004	13.996
2	19.7	14.006	13.993
2.5	22.4	14.007	13.990
3	24.6	14.009	13.988
4	28.6	14.011	13.984
5	31.7	14.013	13.980
6	34.1	14.014	13.978
8	38.1	14.017	13.973
10	41.8	14.019	13.969
12	45.1	14.021	13.965

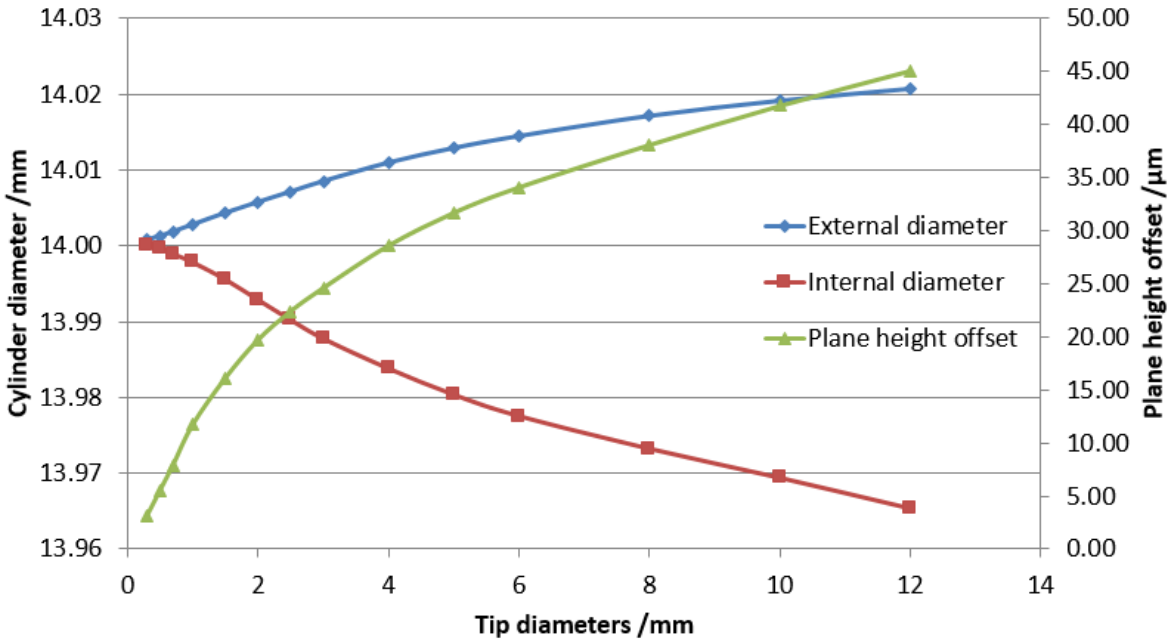

Figure 11. Plane height offsets and cylinder diameters vary in response to disk probe diameters.

4.3 Simulation: varying surface roughness

In the varying surface roughness simulation, the probe disk diameter is fixed (set to 4 mm in this simulation), while the seven examined surfaces vary in their roughness ranging from 0.9 µm to 37.5 µm. These surfaces are measured from the casting Rubert Plate which has a similar surface texture to that of AM processed surfaces. The simulated result of using the morphological method is listed in Table 5 and plotted in Figure 12. It is shown that the rougher the surface texture, the larger offset the disk probe produces for both the plane height and external/internal diameters. However, even for the roughest surface, the offset obtained from the simulation is much smaller than *Pp*, being only 6%~16% of *Pp*.

Table 5. Plane height offset and external/internal cylinder diameters in response to roughness parameters.

***Pa* /µm**	***Pp* /µm**	**Plane height offset /µm**	**External cylinder diameter /mm**	**Deviation /µm**	**Internal cylinder diameter /mm**	**Deviation /µm**
0.9	3.4	0.2	14.000	0	14.000	0
2.5	11.3	1.6	14.001	1	13.999	-1
4.3	18.0	2	14.001	1	13.999	-1
7.0	40.8	2.8	14.001	1	13.999	-1
11.8	42.5	5.2	14.002	2	13.997	-3
23.1	103.7	10.9	14.003	3	13.996	-4
37.5	198.1	31.2	14.012	12	13.981	-19

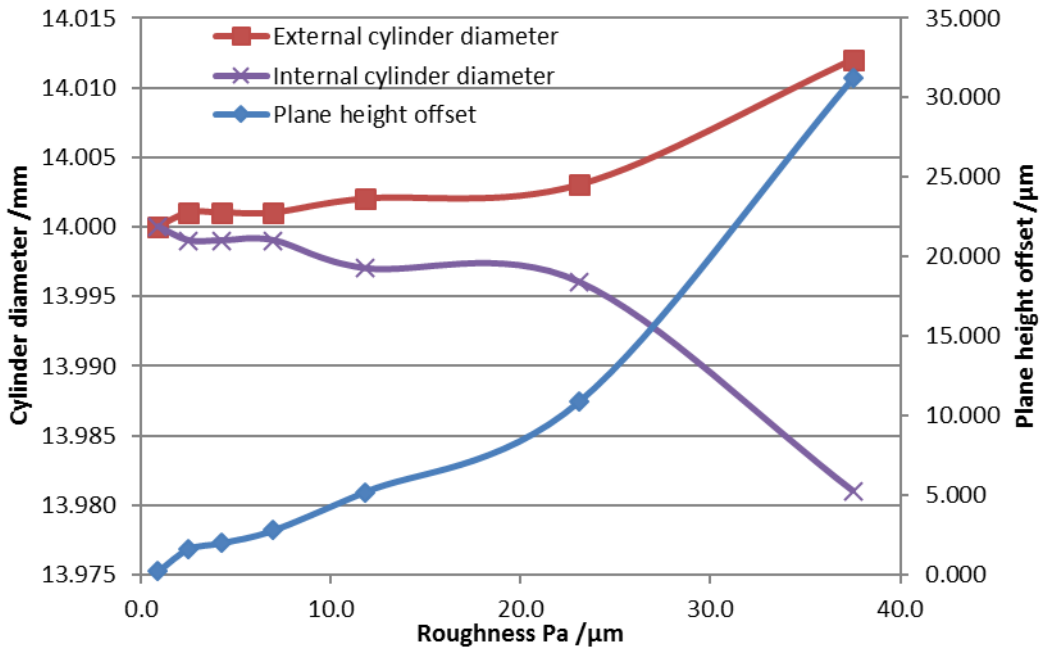

Figure 12. Plane height offset and external/internal cylinder diameter vary in response to surface roughness.

5. Comparison and discussion

The NPL test object was measured by XCT to provide a comparison with the tactile CMM measurement. The XCT 3D reconstruction was checked for scaling issues by using the three ceramic tooling balls. It has been assumed that though the effects of probing a perfect sphere may change the diameter of the sphere, it will not influence the position of the sphere centre. It was therefore assumed that comparing the centre to centre distances of the tooling spheres calculated from the CMM measurements and the XCT measurements, will be the same. This assumption was used to check the XCT data, for scale error, and in this case was found to be insignificant, requiring no correction.

The comparison of tactile CMM (stylus probe tip diameter 3 mm) and XCT on measuring cylinder diameters at eight heights is listed in Table 6. To compensate the CMM probe's mechanical filtering effect, the morphological method is applied to the XCT generated circumference profiles. "XCT1 Diam", "XCT2 Diam" and "XCT3 Diam" in Table 6 refer to the external cylinder diameters resulted from the raw XCT measurement, the XCT data modified by applying the morphological method with the disk probe diameter 3 mm and the XCT data modified by applying the morphological method with the infinite large disk probe diameter (i.e. convex hull). The experimental results show that the deviations between CMM and XCT are close to the *Pp* value 211.9 µm. Assuming that XCT results are more accurate than CMM measurements (Brown et al. 2016; Carmignato et al. 2017), the application of the morphological method to "compensate" the CMM mechanical filtering effect can only reduce a limited number of deviations, see the second from last column of Table 6. Using the convex hull point to enable the maximum compensation can compensate up to a quarter of the deviation. See Figure 13 as an example of illustrating the comparison of the CMM and XCT measurement, cylinder diameters measured at the height of 68 mm.

The results of applying the morphological method on XCT data indicate that the actual deviation between tactile CMM and XCT when measuring AM cylinder diameters is larger than the offset that can be caused by the mechanical filtering effect of the stylus probe. This fact implies that the deviation due to the mechanical filtering effect contributes to a portion of the actual deviation but not all and there are other error sources. Tactile measurements are influenced by such factors as scanning speed and the probe force. It is also a fact that the morphological method is applied to the profile data. Surfaces are three-dimensional and so is the probing tip. The surface topography in the neighbourhood will have an impact on the measurements. Thus the mechanical filtering effect of the stylus probe on areal data should be more significant than that of the profile data. With reference to the XCT measurement, more research is needed to investigate how XCT measurement will shift from the reference.

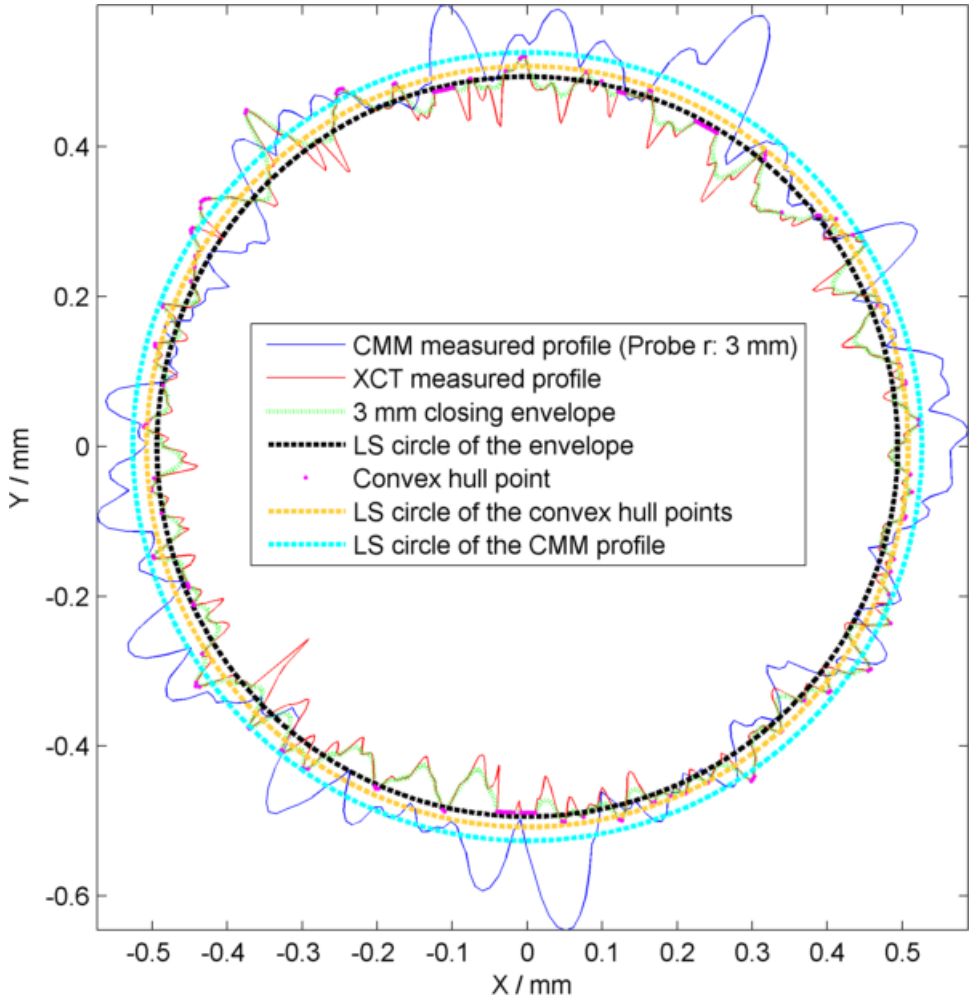

Figure 13. Comparison of the circumference profile resulted from CMM and XCT measurements.

Table 6. Comparison of the cylinder diameters resulted CMM measurement, XCT measurement and applying the morphological method to XCT measurement (Unit: mm).

Height	CMM Diam	XCT1 Diam (Raw)	CMM - XCT1	XCT2 Diam (3 mm probe disk)	CMM - XCT2	XCT3 Diam (convex hull)	CMM - XCT3	XCT2 -XCT1	XCT3 - XCT1
23.5	13.721	13.978	-0.257	13.961	-0.240	13.926	-0.206	-0.017	-0.052
26	13.716	13.968	-0.252	13.942	-0.226	13.893	-0.177	-0.026	-0.075
28.5	13.727	13.975	-0.248	13.958	-0.231	13.923	-0.196	-0.017	-0.052
31	13.755	13.972	-0.217	13.956	-0.201	13.914	-0.159	-0.016	-0.058
68	14.052	13.853	0.199	13.865	0.187	13.893	0.159	0.012	0.040
70.5	14.040	13.855	0.185	13.868	0.172	13.895	0.145	0.013	0.040
73	14.060	13.858	0.202	13.868	0.192	13.898	0.162	0.010	0.040
75.5	14.056	13.848	0.208	13.870	0.186	13.884	0.172	0.022	0.036

6. Conclusion and future work

AM processes tend to produce relatively rough surfaces. The mechanical filtering effect of tactile measurement can be prominent when measuring AM rough surfaces. The use of tactile measurement (e.g. CMM) as a dimensional reference, as is often the case for XCT dimensional measurements, can be limited. Experimental work measuring the plane height offset (distance) and the cylinder diameter (dimension) of the NPL test object using different probe diameters shows that larger probe diameters have stronger mechanical filtering effect. The numerical simulation was also developed using the morphological method based on the Alpha shape theory, which allows a single influence factor to be investigated, e.g. the probe diameter in this work. The simulation results of varying disk probe diameters follow the same pattern as that of the experimental work. For cylinder diameter measurement, the maximum measurement errors caused by the probe mechanical effect are determined by the convex hull points, which is equivalent to using an infinitely large diameter disk probe. Other simulation results using various surface roughness's imply that the rougher the surface is, the greater the influence it will have. The CMM and XCT results of measuring the cylinder diameters of the test object are compared. The morphological method can be applied to XCT measurement data in order to "compensate" the CMM mechanical filtering effect when taking the CMM results as the references. The deviations between CMM and XCT experimental results are at the scale of *Pp*. Morphological compensation can reduce a small portion of this deviation, which suggests that there may be other factors that contribute to these deviations.

A key future work is the investigation of the Gaussian-like low-passing filtering effect caused by the partial volume effect of the XCT system. The proposed work is expected to produce a more reliable dimensional measurement of AM parts. Another consideration of future work is the re-entrant features of AM surfaces, which will influence the measurement and characterisation of AM surface texture, and thus the evaluation of deviation between tactile CMM and XCT.

Acknowledgement

The authors would like to personally thank their colleagues for their assistance and due diligence throughout this work. In particular they would like to thank, from NPL: S. Woodward, A. Sharpe and M. Dury. From NPL, the work was supported by the National Measurement System. From Huddersfield University, the authors gratefully acknowledge the UK's Engineering and Physical Sciences Research Council (EPSRC) funding of the Future Advanced Metrology Hub (EP/P006930/1). S. Lou would like to thank the EPSRC (Grants EP/S000453/1) for funding this work.

Reference

Aloisi V., Carmignato S., Influence of surface roughness on x-ray computed tomography dimensional measurements of additive manufactured parts, Case Stud. Nondestr.Test. Eval., 6 (2016) 104-110.

Bartscher M., Neukamm M., Koch M., Neuschaefer-Rube U., Performance assessment of geometry measurements with micro-ct using a dismountable work-piece-near reference standard, 10th European Conference on Non-Destructive Testing, Moscow, Russia.

Boeckmans B., Tan Y., Welkenhuyzen F., Guo Y.S. Dewulf, W. Kruth J. –P., Roughness offset differences between contact and non-contact measurements, Proceedings of the 15th Euspen International Conference, (2015) 189-190.

Brown S., Sun W. McCarthy M. B., Woolliams P., Assessment of dimensional measurement tools to measure additively manufactured metallic parts, Proceedings of ASPE Summer Topical Meeting: Dimensional Accuracy and Surface Finish in Additive Manufacturing (2016) 200-205.

Carmignato S., Accuracy of industrial computed tomography measurements: experimental results from an international comparison, CIRP Ann. 61 (2012), 491-494.

Carmignato S., Aloisi V., Medeossib F., Zaninia F., Savio E., Influence of surface roughness on computed tomography dimensional measurements, CIRP Ann. 66 (2017) 499-502.

Carmignato, S., Dewulf, W., Leach, R. (Eds.), Industrial X-ray computed tomography. Springer 2018.

Christoph R., Neumann H.J., Multisensor coordinate metrology, Coordinate measuring machines and systems (2nd ed.) 2012 125-152.

Dagnall H., Exploring Surface Texture Taylor Hobson 1998.

Heijmans H. J. A. M., Mathematical morphology: a modern approach in image processing based on algebra and geometry, SIAM Rev. 37 (1995) 1-36

ISO 10360-2 Geometrical product specifications (GPS) -- Acceptance and reverification tests for coordinate measuring machines (CMM) -- Part 2: CMMs used for measuring linear dimensions, 2009.

ISO 14406 Geometrical Product Specifications (GPS) – Extraction, 2003.

ISO 3274 Geometrical Product Specifications (GPS) – Surface texture: Profile method – Nominal characteristics of contact (stylus) instruments, 1996.

ISO 4287 Geometrical Product Specifications (GPS) -- Surface texture: Profile method -- Terms, definitions and surface texture parameters, 1997.

Kruth, J. P., Bartscher, M., Carmignato, S., Schmitt R., De Chiffre L., Weckenmann A., Computed Tomography for Dimensional Metrology, CIRP Ann. 60 (2011) 821-842.

Krystek M., Morphological filters in surface texture analysis, XIth international colloquium on surfaces (2004) 43-55.

Leach R., Haitjema H., Bandwidth characteristics and comparisons of surface texture measuring instruments, Meas. Sci. Technol., 21 (2010) 032001.

Lonardo P.M., Lucca D.A., Chiffre L.D. Emerging Trends in Surface Metrology, Annals of the CIRP, 51 (2002) 701-723.

Lou S., Jiang X., Scott P. J., Applications of morphological operations in surface metrology and dimensional metrology, J. Phys. Conf. Ser. 483 (2014a) 012020.

Lou S., Jiang X., Scott P. J., Geometric computation theory for morphological filtering on freeform surfaces, Proc. R. Soc. London, Ser. *A* 469 (2013) 20130150.

Lou S., Jiang X., Scott P. J., Morphological filters for functional assessment of roundness profiles, Meas. Sci. Technol., 6 (2014b) 065005.

Novak A. H., Runje B. 2017 Influence of object surface roughness in CT dimensional measurement, 7th Conference on Industrial Computed Tomography, Leuven, Belgium.

Qian X., Villarrubia J.S., General three-dimensional image simulation and surface reconstruction in scanning probe microscopy using a dexel representation, Ultramicroscopy, 108 (2007) 29-42

Roger S., Dietzsch M., Gerlach M., Jeβ S., “Real mechanical profile” – the new approach for nano-measurement J. Phys.: Conf. Ser. 13 (2005) 13-9.

Salzinger M., Hornberger P., Hiller J., Analysis and comparison of the surface filtering characteristics of computed tomography and tactile measurement, 6th Conference on Industrial Computed Tomography, Wels, Austria, 2016.

Schmitt R., Niggemann C., Uncertainty in measurement for x-ray-computed tomography using calibrated work pieces, Meas. Sci. Technol., 21 (2010) 054008.

Soret M, Bacharach SL, Buvat I., Partial-volume effect in PET tumor imaging, J. Nucl. Med. 48 (2007) 932–45.

Thomas, T. R., Rough Surfaces, London, UK: Imperial College Press, 1999.

Villarrubia J. S. Algorithms for scanned probe microscope, image simulation, surface reconstruction and tip estimation. J. Nat. Ins.t Stand and Technol. 102 (1997) 435–454

Volume Graphics, VGStudio Max 2.0 Reference Manual 2.0, www.volumegraphics.com

Weckenmann A., Estler T., Peggs G., McMurtry D., Probing systems in dimensional metrology, CIRP Ann. 53 (2004) 657-684.

Whitehouse D., Surfaces and Their Measurement, Hermes Penton Science, 2002.

Worring M. and Smelders W. M., Shape of arbitrary finite point set in R2, J. Math. Image Vis. 4 (1994) 151-170.